A Novel Calculation Method for Iron Loss Resistance Suitable in Modeling Permanent-Magnet Synchronous Motors

Naomitsu Urasaki, *Member, IEEE*, Tomonobu Senjyu, *Member, IEEE*, and Katsumi Uezato

***Abstract*—This paper proposes a calculation method for iron loss resistance, suitable for modeling permanent-magnet synchronous motors. The proposed method is based on the linear feature between semi-input power and square of speed electromotive force. The iron loss resistance is calculated from the slope of this linear function in the offline manner. The advantage of the proposed method is that the iron loss resistance can be calculated directly without any measurements related to mechanical loss. In addition, the proposed method can be executed at any load conditions. The validity of the proposed method is experimentally confirmed by the comparison between the actual torque and the calculated torque containing the iron loss resistance.**

***Index Terms*—Iron loss resistance, modeling, parameter calculation, parameter mismatch, permanent-magnet synchronous motor.**

I. Introduction

IN RECENT YEARS, vector-controlled ac motors, such as induction motor, permanent-magnet synchronous motor (PMSM), and synchronous reluctance motor, have become standard in industrial drives and their performance improvement is an important issue. Particularly, improvement of control performance and drive efficiency is essentially required for drives used in electric vehicles. Conventional vector control strategies have been implemented under the assumption that there is no iron loss in motors. However, in reality, there is a certain amount of iron loss, now small it may be, that influences the flux linkage and output torque of the motors. In order to improve not only the drive efficiency but also control performance, it is necessary to compensate for this iron loss influence on vector-controlled drives [1]. For this reason, several authors have made an attempt to consider the iron loss in vector controlled ac motor drives [2]–[16]. These methods use an equivalent circuit, in which iron loss resistance is inserted in parallel with the magnetizing branch and speed electromotive force (emf). According to this mathematical model, the output torque is strictly proportional to magnetizing currents. From the perspective of improving the torque control, the output torque should be controlled by the magnetizing currents. Since the magnetizing currents cannot be detected directly from the terminal quantities, they are indirectly calculated using the line currents and the iron loss resistance [3], [5], [9], [17]. On the other hand, from the improvement of the drive efficiency point of view, the iron loss resistance is indispensable for the efficiency control strategies [17]–[20]. Thus, it is necessary to compute the iron loss resistance to achieve the accurate vector control performance.

An online identification of the iron loss resistance [11] and adaptive iron loss compensation techniques [12], [13] are developed for induction motor drives. However, in the online identification methods, it is difficult to include mechanical loss. As a result, the accuracy on the iron loss resistance is degraded. It is well known that the iron loss is a part of no-load loss in an ac motor drive and it is obtained by subtracting a mechanical loss from the no-load loss in the offline manner. A general method for dividing the no-load loss into the iron loss and mechanical loss uses the characteristic curve of the no-load loss versus input voltage. In this method, the no-load loss at zero input voltage is assumed to be the mechanical loss and the iron loss is calculated by subtracting the mechanical loss from the no-load loss. However, since the no-load loss at zero input voltage cannot be measured directly, it is estimated by the interpolation of the characteristic curve in low input voltage area. The iron loss resistance is calculated from the obtained iron loss. The disadvantage of this method is that the interpolation is undetermined. Further, any error involved in the measurement of mechanical loss (offset the estimated iron loss) leads to over or underestimation of iron loss resistance. Although this problem can be resolved by using an auxiliary motor [21], it is restricted only to the particular application.

This paper proposes a novel calculation method for the iron loss resistance useful for modeling of PMSM. The iron loss resistance is calculated based on the linear feature between semi-input power and square of speed emf in the offline manner. Here, the semi-input power means the power which is calculated by subtracting the copper loss from the input power (i.e., the semi-input power is equivalent to the sum of the no-load loss and the mechanical output power under load conditions), while the semi-input power is equivalent to the no-load loss only under a no-load condition. As compared with the conventional method, the measurement data are the same (i.e., the input power, input voltage, and input current), while the manipulation of the measurement data is peculiar. First, the semi-input power and the square of speed emf are calculated from the measurement data. Then, the characteristic of the semi-input power versus the square of speed emf is plotted. The characteristic appears as a linear and its slope is equal to the inverse of the

Manuscript received January 22, 2001; revised May 4, 2002.

The authors are with the Department of Electrical and Electronic Engineering, University of the Ryukyus, Okinawa 903-0213, Japan (e-mail: urasaki@tec.u-ryukyu.ac.jp).

Digital Object Identifier 10.1109/TEC.2002.808329

iron loss resistance and its vertical axis (y-axis) intercept corresponds to the sum of the mechanical output power and loss. Of course, the mechanical output power is not included in the intercept under the no-load condition. Since the proposed method uses only the slope, the iron loss resistance can be directly calculated without the measurement of mechanical loss. In addition, the proposed method can be used for any load conditions as long as the load is kept constant during measurement. As the conventional method, the proposed method also suffers from the parameter mismatch of the armature resistance. In this paper, the possible countermeasures, which could be taken to relieve the influence of the parameter mismatch, are investigated. The validity of the proposed method is confirmed by the comparison between the actual torque and the calculated torque containing the iron loss resistance.

This paper is organized as follows. Mathematical formulation of PMSM including iron loss is presented in Section II. The proposed measurement method is explained in Section III. Experimental results are discussed in Section IV. Influence of the armature resistance mismatch and its countermeasure are investigated in Section V. The validity of the proposed method is confirmed in Section VI. Conclusions are given in the final section.

II. Mathematical Formulation of PMSM Taking Iron Loss Into Account

In the synchronous reference frame (d–q), the voltage equations for PMSM are expressed as

$$\left.\begin{aligned} v_d &= Ri_d + p\Psi_d - \omega_e\Psi_q \\ v_q &= Ri_q + p\Psi_q + \omega_e\Psi_d \end{aligned}\right\} \tag{1}$$

where the first term on the right-hand side represents the voltage drop for the armature resistance R, and the second and third terms represent the transformer emf and speed emf, respectively.

Fig. 1 shows the d–q axes equivalent circuits of PMSM [18] which are traditionally used when the iron loss is considered. In this circuit, an iron loss resistance R_i is inserted in the parallel fashion. Thus, the d–q axes line currents (i_d, i_q) are divided into iron loss currents (i_{di}, i_{qi}) and magnetizing currents (i_{dm}, i_{qm}). In this equivalent circuit, the iron loss P_i due to iron loss resistance is modeled as an equivalent copper loss as

$$P_i = R_i(i_{di}^2 + i_{qi}^2). \tag{2}$$

In the steady state, the iron loss currents are expressed as

$$\left.\begin{aligned} i_{di} &= -\frac{\omega_e\Psi_q}{R_i} \\ i_{qi} &= \frac{\omega_e\Psi_d}{R_i} \end{aligned}\right\}. \tag{3}$$

Substituting (3) into (2) results in the following equation:

$$P_i = \frac{\omega_e^2(\Psi_d^2 + \Psi_q^2)}{R_i}. \tag{4}$$

From (4), it can be noted that the iron loss depends on the electrical angular velocity ω_e and flux linkages (Ψ_d and Ψ_q). The flux linkage equations for PMSM are given as

$$\left.\begin{aligned} \Psi_d &= Li_{dm} + K_e \\ \Psi_q &= Li_{qm} \end{aligned}\right\} \tag{5}$$

where L is the armature inductance and K_e is the emf constant. The output torque is calculated from the vector product of the flux linkages and magnetizing currents as

$$\begin{aligned} \tau &= P(\Psi_d i_{qm} - \Psi_q i_{dm}) \\ &= PK_e i_{qm} \end{aligned} \tag{6}$$

where P is the number of pole pairs. As can be seen from (6), the output torque is proportional to the q-axis magnetizing current. Thus, it is necessary to control the magnetizing current in order to control the output torque exactly. However, since the magnetizing current cannot be obtained directly from the terminal quantities, this paper uses the following procedure [22].

The magnetizing currents are the difference between the line currents and iron loss currents given by

$$i_{dm} = i_d + \frac{\omega_e L}{R_i} i_{qm} \tag{7}$$

$$i_{qm} = i_q - \frac{\omega_e L}{R_i}\left(i_{dm} + \frac{K_e}{L}\right). \tag{8}$$

Substituting (7) into (8), gives the q-axis magnetizing current as

$$i_{qm} = \frac{1}{1 + \left(\frac{\omega_e L}{R_i}\right)^2}\left\{i_q - \frac{\omega_e L}{R_i}\left(i_d + \frac{K_e}{L}\right)\right\}. \tag{9}$$

Here, an assumption, iron loss resistance R_i is much greater than reactance $\omega_e L$, is used

$$\left(\frac{\omega_e L}{R_i}\right)^2 \ll 1. \tag{10}$$

The validity of this assumption is confirmed in Section IV. Applying (10) to (9) results

$$i_{qm} = i_q - \frac{\omega_e L}{R_i}\left(i_d + \frac{K_e}{L}\right). \tag{11}$$

Here, the line currents (i_d and i_q) can be obtained directly from the terminal quantities, then the q-axis magnetizing current can be easily calculated from (11).

On similar lines, the d-axis magnetizing current can be obtained, and it is expressed as

$$i_{dm} = i_d + \frac{\omega_e L}{R_i}\left(i_q - \frac{\omega_e K_e}{R_i}\right). \tag{12}$$

As can be seen from (11) and (12), the iron loss resistance R_i is necessary to calculate the magnetizing currents in addition to the conventional PMSMs' parameters, such as the armature inductance L and emf constant K_e. This paper proposes a calculation method for this iron loss resistance.

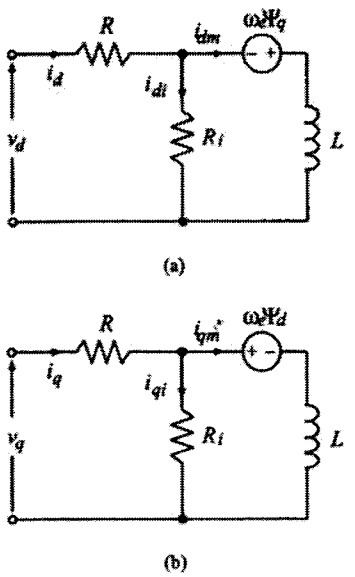

Fig. 1. d–q axes equivalent circuits for PMSM taking iron loss into account. (a) d-axis. (b) q-axis.

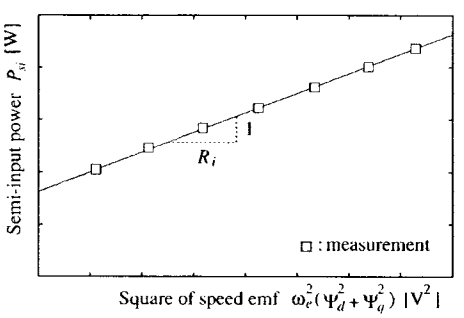

Fig. 2. Image of the characteristics of semi-input power versus square of speed emf.

III. Calculation Method for Iron Loss Resistance

In the steady state ($p = 0$) and from (1)–(5), the input power P_{in} is expressed as

$$\begin{aligned} P_{in} &= v_d i_d + v_q i_q \\ &= R(i_d^2 + i_q^2) + \frac{\omega_e^2(\Psi_d^2 + \Psi_q^2)}{R_i} + \omega_e K_e i_{qm} \end{aligned} \quad (13)$$

where the first term is the copper loss P_c, the second term is the iron loss P_i, and the third term is the output power P_{out}. According to this formulation, the semi-input power P_{si}, which is defined as the power calculated by subtracting the copper loss from the input power, corresponds to the sum of the iron loss and output power as

$$\begin{aligned} P_{si} &= P_i + P_{out} \\ &= \frac{1}{R_i}\omega_e^2(\Psi_d^2 + \Psi_q^2) + P_{out}. \end{aligned} \quad (14)$$

In practice, the output power essentially includes mechanical and stray losses. In the proposed method, measurements of the mechanical loss and stray loss are not required because the iron loss resistance is calculated using only the first term in (14). Note that the proposed method implicitly includes the mechanical loss and stray loss although the mechanical loss and stray loss are never expressed explicitly.

When both the rotor speed and load torque are constant, the output power P_{out} is also constant, it is because the mechanical, stray losses, and the pure mechanical output power terms are constants. Then, the semi-input power can be regarded as the linear function of the square of the speed emf ($\omega_e^2(\Psi_d^2 + \Psi_q^2)$), emphasized in (14). In this situation, the slope of this linear function corresponds to the inverse of the iron loss resistance ($1/R_i$) and the intercept corresponds to the output power P_{out}. The iron loss resistance R_i is calculated, employing the following procedure.

1) Operates the PMSM under constant speed and load conditions.
2) By changing the d-axis current i_d, set of input power P_{in}, input voltage V_{rms}, and input current I_{rms} measurements were recorded. Note that the change in d-axis current will influence only the flux linkage but not the output torque;
3) Using the measured data obtained in step 2, the semi-input power and the square of speed emf are calculated from the following expressions:

$$\begin{aligned} P_{si} &= P_{in} - R(i_d^2 + i_q^2) \\ &= P_{in} - 3RI_{rms}^2 \end{aligned} \quad (15)$$

$$\begin{aligned} \omega_e^2(\Psi_d^2 + \Psi_q^2) &= (v_q - Ri_q)^2 + (v_d - Ri_d)^2 \\ &= V_{rms}^2 - 2RP_{in} + 3R^2 I_{rms}^2 \end{aligned} \quad (16)$$

where $V_{rms} = \sqrt{v_d^2 + v_q^2}$, $I_{rms} = \sqrt{i_d^2 + i_q^2}/\sqrt{3}$.

4) The linear characteristic semi-input power versus the square of speed emf is plotted as shown in Fig. 2.
5) The slope of this linear function is obtained with the least squares method. The neighborhood of operating point $i_d = 0$ is linearized in order to avoid the influence of the armature resistance mismatch and magnetic saturation. (Discussion is given in Section V.)
6) The iron loss resistance R_i is calculated from the inverse of the slope obtained in step 5.

The advantage of the proposed method is that the iron loss resistance can be directly calculated without measuring the mechanical loss. In addition, this method can be used at any load, provided the load is kept constant during measurement. The disadvantage of this method is that the parameter mismatch in the armature resistance R. The influence of this armature resistance mismatch and its countermeasures are discussed in Section V.

IV. Calculation Results for Iron Loss Resistance

Fig. 3 shows the experimental setup for the proposed method. The specifications of the tested PMSM employed in this experiment are listed in Table I. The electrical input power applied to the tested PMSM is supplied through the voltage source inverter (VSI) [i.e., dc-link voltage, carrier frequency, and dead time are 150 V, 5 kHz, and 5 μs, respectively]. The electrical input power P_{in}, input voltage V_{rms}, and input current I_{rms} are measured with the help of a digital power meter (DPM). In order to keep the rotor speed constant, a speed feedback control is used.

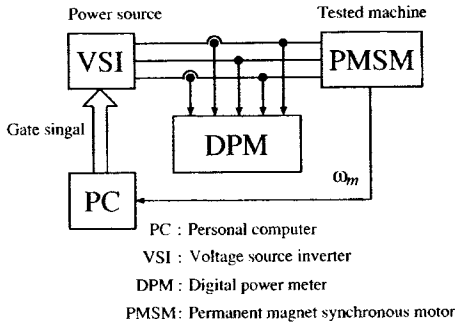

Fig. 3. Experimental system.

TABLE I
MOTOR SPECIFICATIONS

rated power	P_n	160 W
rated torque	τ_n	0.5 N·m
rated speed	N_n	3,000 rpm
armature resistance	R	2.14 Ω
armature inductance	L	0.0079 H
emf coefficient	K_e	0.0658 V·s/rad
number of pole pairs	P	2

Fig. 4 shows the semi-input power versus the square of speed emf for the no-load condition at speed of 2000 r/min when the d-axis current is changed from +3.5 A to −3.5 A. As can be confirmed from Fig. 4(a), the square of speed emf decreases with decreasing the d-axis current. Since the square of speed emf is a quadratic equation with variable d-axis current, variation in the square of speed emf is enlarged by magnetizing operation ($i_d > 0$) and reduced by demagnetizing operation ($i_d < 0$). In addition, it confirms that the output torque is almost kept constant irrespective of changing the d-axis current, it is because the q-axis current is kept constant. As can be seen from Fig. 4(b), the semi-input power is almost proportional to the square of speed emf. Thus, the characteristic of the semi-input power versus the square of speed emf can be approximate as a linear function. This characteristic is linearized in the neighborhood of nominal operating point for PMSM [i.e., $i_d = 0$ (minimum copper loss, P_c, condition)], because the influence of the armature resistance mismatch and magnetic saturation is serious at the extreme demagnetizing and magnetizing points. After linearization, the iron loss resistance R_i for no-load condition at 2000 r/min is straightforwardly calculated from the slope of this linear function.

Fig. 5 shows the semi-input power versus the square of speed emf for various load conditions at 2000 r/min. All of the characteristics are linear and their slopes are almost the same (i.e., the iron loss resistance is almost the same, irrespective of load conditions). Of course, the intercept increases with increasing load torque, because it corresponds to the output power.

Similar calculations have been made for different rotor speeds from 750 to 3000 r/min. Fig. 6 shows calculated results for the iron loss resistance obtained for different rotor speeds. As can be seen from Fig. 6(a), the iron loss resistance is almost proportional to the rotor speed. The linear characteristic of the iron loss resistance qualitatively agrees with the results obtained in the literature [12]–[14]. Fig. 6(b) shows the square of impedance

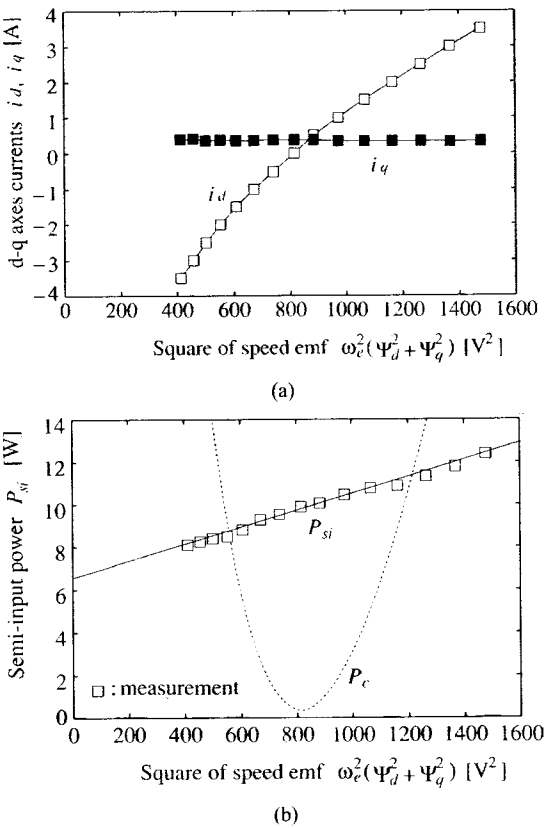

Fig. 4. Semi-input power versus square of speed emf. (a) d–q axes currents. (b) Semi-input power.

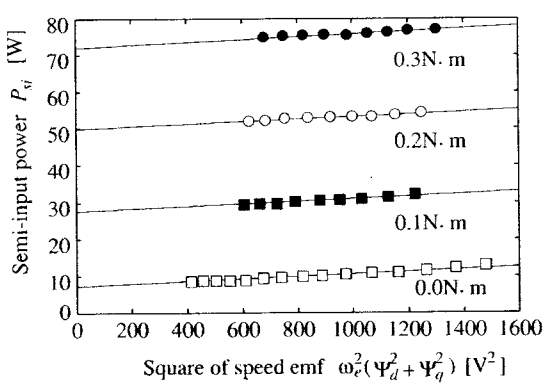

Fig. 5. Semi-input power versus square of speed emf for various load condition.

ratio $(\omega_e L/R_i)^2$ versus rotor speed. The ratio is calculated by using the iron loss resistance shown in Fig. 6(a). Since the order of the ratio is 10^{-4}, the relation introduced in (10) is valid.

Fig. 7 shows the iron loss P_i and output power P_{out} for the flux linkage under the no-load condition. The iron loss is calculated by using (4), while the output power is calculated by subtracting the iron loss from the semi-input power. The iron loss increases with increasing the flux linkage, while the output power is almost constant with respect to flux linkage. Note that, because of the existence of mechanical loss and stray loss, the output power P_{out} is not equal to zero, despite the no-load condition. It can be confirmed from Fig. 7 that the semi-input power indicated in (14) is appropriately divided into the iron loss and the output power.

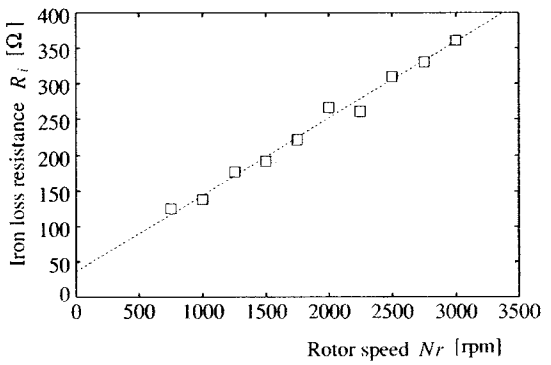

(a)

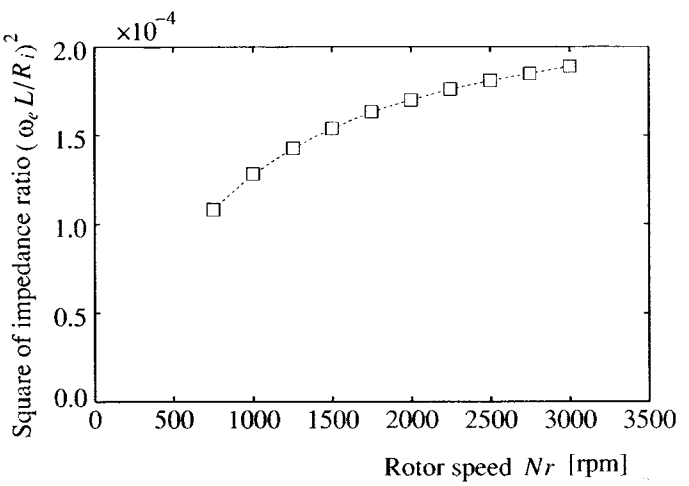

(b)

Fig. 6. Characteristics of iron loss resistance for rotor speed. (a) Iron loss resistance. (b) Square of impedance ratio.

V. Influence of Armature Resistance Mismatch

In the proposed method, the armature resistance R is used in the calculation of both the semi-input power and the square of speed emf. Then, the parameter mismatch of the armature resistance leads to wrong characterization of the semi-input power versus square of speed emf. As a result, error is involved in the calculation of the iron loss resistance. In this section, the influence of the armature resistance mismatch on the calculation of the iron loss resistance is investigated.

When the error for the armature resistance is ΔR, the semi-input power is expressed as

$$P'_{si} = P_{in} - 3(R + \Delta R)I^2_{rms}. \tag{17}$$

From (15) and (17), the calculation error for the semi-input power $E_{psi}(=P'_{si} - P_{si})$ is obtained as

$$E_{psi} = -3\Delta R I^2_{rms}. \tag{18}$$

It can be seen from (18) that the error E_{psi} increases with increasing the input current I_{rms}.

On the similar lines, the square of the speed emf with the armature resistance mismatch ΔR is expressed as

$$\omega_e^2(\Psi_d^2+\Psi_q^2)' = V^2_{rms} - 2(R + \Delta R)P_{in} + 3(R + \Delta R)^2 I^2_{rms}. \tag{19}$$

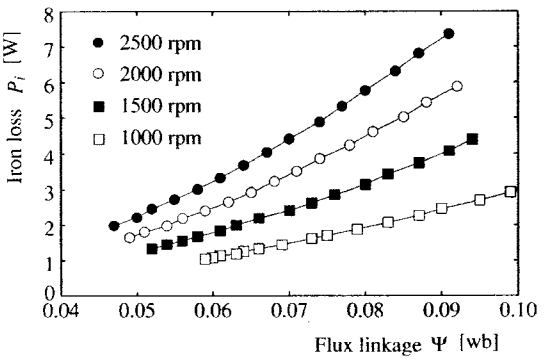

(a)

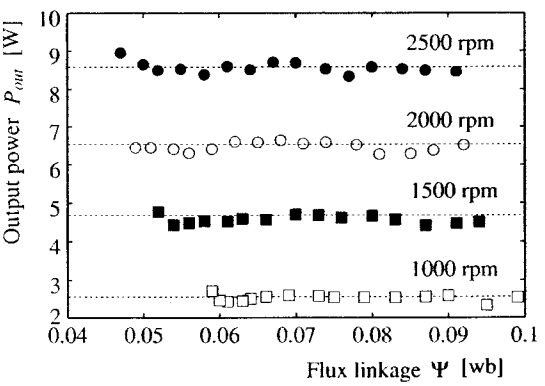

(b)

Fig. 7. Iron loss and output power with respect to flux linkage under no-load condition. (a) Iron loss. (b) Output power.

From (16) and (19), the calculation error for the square of speed emf E_{sse} $(=\omega_e^2(\Psi_d^2 + \Psi_q^2)' - \omega_e^2(\Psi_d^2 + \Psi_q^2))$ is obtained as

$$E_{sse} = \Delta R\{3(2R + \Delta R)I^2_{rms} - 2P_{in}\}. \tag{20}$$

It can be seen from (20) that the error E_{sse} also increases by increasing the input current I_{rms}.

Fig. 8(a) and (b) shows the characteristics of semi-input power versus the square of speed emf for no-load condition and 0.2 N · m at 2000 r/min, respectively. The error ±10% of the rated armature resistance is considered. As can be expected from (18) and (20), the calculation error increases with increasing input current (i.e., the absolute value of the d-axis current. As a result, the characteristics are no longer linear. However, the neighborhood of $i_d = 0$ operating point yields a linear characteristic. In addition, the slopes are almost the same despite the parameter mismatch. Accordingly, the influence of the armature resistance mismatch can be relieved by linearizing the characteristic in the neighborhood of $i_d = 0$ operating point.

VI. Validity of Calculation Results

In order to confirm the validity of the calculation for the iron loss resistance, the calculated torque containing the iron loss resistance is compared with the actual torque. To verify the accuracy of the iron loss resistance, the calculated torque ignoring the iron loss is also plotted.

Fig. 9 shows the electromagnetic torque versus q-axis current at 2000 r/min. In this figure, measurements denote the actual torque which is obtained with the help of torque transducer. The

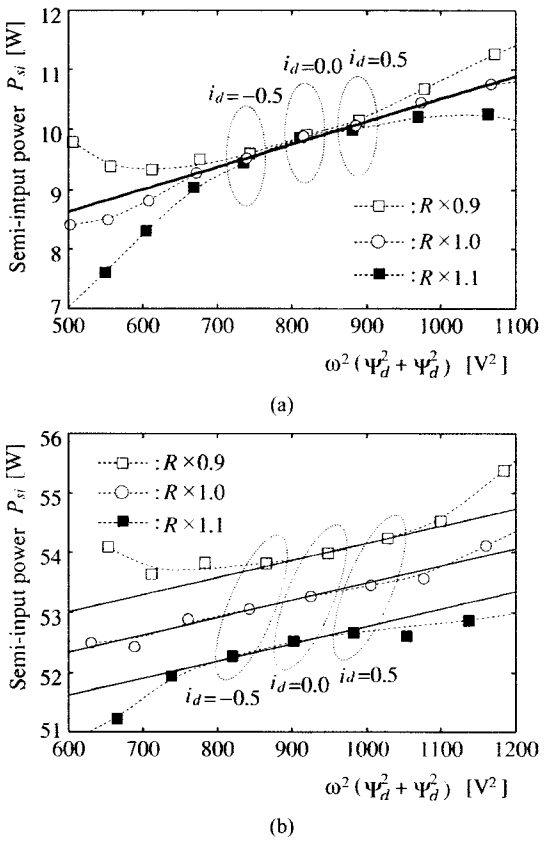

Fig. 8. Semi-input power versus square of speed emf under ±10% armature resistance error. (a) No-load condition. (b) Load condition (0.2 · m).

two lines denote the calculated torques and these are calculated by

$$\tau_{cal} = PK_e\left\{i_q - \frac{\omega_e L}{R_i}\left(i_d + \frac{K}{L}\right)\right\} \tag{21}$$

where $R_i = \infty$, when the iron loss is ignored. In all cases, the d-axis current i_d is kept at zero. As can be seen from Fig. 9, the calculated torque with proposed calculation method (solid line) agrees well with the actual torque, while the calculated torque with $R_i = \infty$ (dotted line) is larger than the actual torque by 2.6% of rated torque. In respect of other rotor speeds, similar results have been obtained. These comparisons confirm the validity of the proposed calculation method for the iron loss resistance used in modeling the PMSM.

VII. Conclusions

This paper has proposed a novel calculation method for the iron loss resistance useful for modeling PMSM. The proposed method is based on the linear characteristic between the semi-input power and the square of speed emf. The iron loss is directly calculated from the slope of this linear function in the offline manner. The advantage of the proposed method is that the iron loss resistance can be directly calculated without measuring mechanical loss. In addition, the proposed method can be used for any load conditions. Although the proposed method suffers from the parameter mismatch of the armature resistance, the countermeasure of this problem has also been investigated. The validity of the proposed method has been experimentally confirmed by the comparison between the actual torque and calculated torque containing the iron loss resistance.

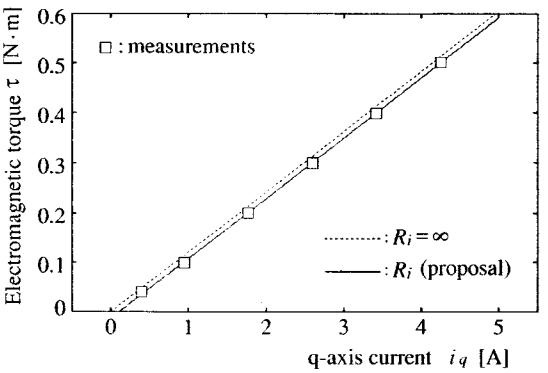

Fig. 9. Electromagnetic torque versus q-axis current.

References

[1] I. Boldea and S. A. Nasar, "Unified treatment of core losses and saturation in the orthogonal-axis model of electrical machines," *Proc. Inst. Elect. Eng.-Elect. Power Applicat.*, pt. B, vol. 134, no. 6, pp. 355–363, Nov. 1987.

[2] L. Xu, X. Xu, T. A. Lipo, and D. W. Novotny, "Vector control of a synchronous reluctance motor including saturation and iron losses," *IEEE Trans. Ind. Applicat.*, vol. 27, pp. 977–984, Sept./Oct. 1991.

[3] L. Xu and J. Yao, "A compensated vector control scheme of a synchronous reluctance motor including saturation and iron losses," *IEEE Trans. Ind. Applicat.*, vol. 28, pp. 1330–1338, Nov./Dec. 1992.

[4] K. Uezato, T. Senjyu, and Y. Tomori, "Modeling and vector control of synchronous reluctance motors including stator iron loss," *IEEE Trans. Ind. Applicat.*, vol. 30, pp. 971–976, July/Aug. 1994.

[5] S.-J. Kang and S.-K. Sul, "Highly dynamic torque control of synchronous reluctance motor," *IEEE Trans. Power Electron.*, vol. 13, pp. 793–798, July 1998.

[6] A. Vagati, M. Pastorelli, G. Franceschini, and V. Drogoreanu, "Flux-observer-based high-performance control of synchronous reluctance motors by including cross saturation," *IEEE Trans. Ind. Applicat.*, vol. 35, pp. 597–605, May/June 1999.

[7] T. Mizuno, J. Takayama, T. Ichioka, and M. Terashima, "Decoupling control method of induction motor taking stator core loss into consideration," in *Proc. IPEC-Tokyo*, Tokyo, Japan, 1990, pp. 69–74.

[8] E. Levi, "Impact of iron loss on behavior of vector controlled induction machines," *IEEE Trans. Ind. Applicat.*, vol. 31, pp. 1287–1296, Nov./Dec. 1995.

[9] E. Levi, M. Sokola, A. Boglietti, and M. Patorelli, "Iron loss in rotor-flux-oriented induction machines: Identification, assessment of detuning, and compensation," *IEEE Trans. Power Electron.*, vol. 11, pp. 698–709, Sept. 1996.

[10] J. Jung and K. Nam, "A vector control scheme for EV induction motors with a series iron loss model," *IEEE Trans. Ind. Electron.*, vol. 45, pp. 617–624, Aug. 1998.

[11] A. Dittrich, "Model based identification of the iron loss resistance of an induction machine," in *Proc. Power Electronics and Variable Speed Drives*, London, U.K., Sept. 1998, IEE Conf. Pub. no. 456, pp. 500–503.

[12] H. Rasmussen, P. Vadstrup, and H. Borsting, "Rotor field oriented control with adaptive iron loss compensation," in *Proc. IAS*, Phoenix, AZ, 1999, no. IDC99-10.

[13] T. Noguchi, P. Nakmahachalasint, and N. Watanakul, "Precise torque control of induction motor with on-line parameter identification in consideration of core loss," in *Proc. PCC*, Nagaoka, Japan, 1997, pp. 113–118.

[14] R. S. Wieser, "Some clarifications on the impact of AC machine iron properties on space phasor models and field oriented control," in *Proc. ICEM*, Istanbul, Turkey, 1998, pp. 1510–1515.

[15] T. Pham-Dinh and E. Levi, "Core loss in direct torque controlled induction motor drives: Detuning and compensation," in *Proc. Power Eng. Soc. Conf.*, Vancouver, BC, Canada, 2001, pp. 1429–1434.

[16] T. Senjyu, T. Shimabukuro, and K. Uezato, "Vector control of synchronous permanent magnet motors including stator iron loss," *Int. J. Electron.*, vol. 80, no. 2, pp. 181–190, 1996.

[17] H.-D. Lee, S.-J. Kang, and S.-K. Sul, "Efficiency-optimized direct torque control of synchronous reluctance motor using feedback linearization," *IEEE Trans. Ind. Electron.*, vol. 46, pp. 192–198, Feb. 1999.
[18] S. Morimoto, Y. Tong, Y. Takeda, and T. Hirasa, "Loss minimization control of permanent magnet synchronous motor drives," *IEEE Trans. Ind. Electron.*, vol. 41, pp. 511–517, Sept./Oct. 1994.
[19] K. Matsuse, T. Yoshizumi, S. Katsuta, and S. Taniguchi, "High-response flux control of direct-field-oriented induction motor with high efficiency taking core loss into account," *IEEE Trans. Ind. Applicat.*, vol. 35, pp. 62–69, Jan./Feb. 1999.
[20] F. F-Bernal, A. G-Cerrada, and R. Faure, "Model-based loss minimization for dc and ac vector-controlled motors including core saturation," *IEEE Trans. Ind. Applicat.*, vol. 36, pp. 755–763, May/June 2000.
[21] A. Boglietti, P. Ferraris, M. Lazzari, and M. Pastorelli, "Influence of the inverter characteristics on the iron loss in PWM inverter-fed induction motors," *IEEE Trans. Ind. Applicat.*, vol. 32, pp. 1190–1194, Sept./Oct. 1996.
[22] N. Urasaki, T. Senjyu, and K. Uezato, "An accurate modeling for permanent magnet synchronous motor drives," in *Proc. APEC 2000*, New Orleans, LA, 2000, pp. 387–392.

Naomitsu Urasaki (M'98) was born in Okinawa Prefecture, Japan, in 1973. He received the B.S. and M.S. degrees in electrical engineering from the University of the Ryukyus, Okinawa, Japan, in 1996 and 1998, respectively.

Currently, he is a Research Associate with the Department of Electrical and Electronic Engineering, Faculty of Engineering, at the University of the Ryukyus, where he has been since 1988. His research interests are in the areas of modeling and control of ac motors.

Mr. Urasaki is a member of the Institute of Electrical Engineers of Japan.

Tomonobu Senjyu (M'02) was born in Saga Prefecture, Japan, in 1963. He received the B.S. and M.S. degrees in electrical engineering from the University of the Ryukyus, Okinawa, Japan, in 1986 and 1988, respectively, and the Ph.D. degree in electrical engineering from Nagoya University, Nagoya, Japan, in 1994.

Currently, he is a Professor with the Department of Electrical and Electronic Engineering, Faculty of Engineering, at the University of the Ryukyus, where he has been since 1988. His research interests are in the areas of stability of ac machines, advanced control of electrical machines, and power electronics.

Dr. Senjyu is a member of the Institute of Electrical Engineers of Japan.

Katsumi Uezato was born in Okinawa Prefecture, Japan, on February 5, 1940. He received the B.S. degree in electrical engineering from the University of the Ryukyus, Okinawa, Japan, in 1963, the M.S. degree in electrical engineering from Kagoshima University, Kagoshima, Japan, in 1972, and the Ph.D. degree in electrical engineering from Nagoya University, Nagoya, Japan, in 1983.

Currently, he is a Professor with the Department of Electrical and Electronic Engineering, Faculty of Engineering, University of the Ryukyus, where he has been since 1972. His research interests are in stability and control of synchronous machines.

Dr. Uezato is a member of the Institute of Electrical Engineers of Japan.